Analytical expression of the refractivity profile. Subrefraction and optical cases

Jacques CLAVERIE
CREC St-Cyr & IETR
Ecoles de St-Cyr Coëtquidan
Guer, France
jacques.claverie@st-cyr.terre-net.defense.gouv.fr

Yvonick HURTAUD
CGN2/SDO
DGA Maitrise de l'Information
Bruz, France
yvonick.hurtaud@intradef.gouv.fr

***Abstract*—The vertical refractivity profile within the Marine Surface Layer is a key parameter to predict the performances of detection sensors (Radars as well as ElectroOptical devices). For practical purposes, it could appear very useful to describe the refractivity profile with an analytical expression. Recently, a new equation, developed for radar applications, was successfully used to approximate the refractivity profiles computed by a physical *bulk* model. In this paper, we extend the analytical formulation to the optical cases dominated by subrefraction situations. Using a ray tracing algorithm and experimental data related to mirage effects, our paper shows that the physical bulk profiles and the fitted analytical ones give very similar results.**

Keywords—RF and EO propagtion; refractive index profile; analytical expression; ray tracing; mirage zones.

I. Introduction

The knowledge of the vertical refractivity profiles is necessary to assess the performances of detection sensors operating at RF frequency bands or at Electro-Optical (EO) wavelengths. Within the Marine Surface Layer (MSL), RF propagation is, most of the time, characterized by the ducting phenomena (resulting in extended detection ranges), meanwhile EO propagation is generally affected by subrefraction (leading to reduced detection ranges and mirage effects). The vertical refractivity profiles within the MSL can be computed by the means of "*bulk*" models applying the Monin-Obukhov similarity theory. To limit the amount of profile data to be stored, the use of analytical approximations of the *bulk* profiles seems to be an interesting approach. Quite recently and dealing with the RF case, Salamon, Hansen and Abbott (SHA) published an expression that generalized the classical log-linear law mainly valid for the near neutral atmospheric situations [1]. We have already shown that this expression was able, with a very good agreement, to fit the profiles derived from PIRAM, the French *bulk* model [2]. The main purpose of this paper is to propose an extension of the SHA formulation to the EO domain.

II. Refrectivity profiles for the RF and EO domains

A. Typical behaviors

As the tropospheric refractive index is very close to unity, the use of the refractivity N is generally preferred. Refractivity is a function of the total atmospheric pressure, the air temperature and of the water vapor pressure. This dependency is not the same for RF and EO bands, the water vapor pressure having much less influence in the EO domain. It is also convenient to use the modified refractivity M, practically defined as (z being the height above the sea level):

$$M(z) = N(z) + 0.157 \cdot z \quad (1)$$

At RF bands, the vertical M profile generally has a minimum value at a height defined as the evaporation duct height (Z_c). At EO wavelengths, subrefraction is the most frequent propagation mode and the vertical N profile has a maximum value at a height arbitrarily denoted $-Z_c$ (Z_c<0) [3]. Z_c represents the Characteristic Refractive Height which definition is summarized by Fig. 1. This definition is also convenient to describe the less common cases: subrefraction for RF bands and ducting in the EO domain.

B. Analytical expressions of the vertical profiles

The original analytical expression proposed by SHA is the following:

$$M(z) = M(0) + G_M \left[z - D_p \frac{\left(\frac{z+z_0}{z_0}\right)^p - 1}{p} \right] \quad (2)$$

where G_M is the modified refractivity gradient that would be reached at an infinite height (with a value usually closed to the standard one of -118 M/km) and z_0 is the roughness length arbitrarily fixed at 0.00015 m. The parameters D_p and p have no physical meaning but are linked to the duct height δ by the relation:

$$D_p = [(\delta + z_0)^{1-p}] \cdot z_0^p \quad (3)$$

As mentioned by the authors of [1], (3) may also be used to describe subrefraction cases. In such a case we prefer to deal with the N vertical profile assuming an analytical expression very similar to (2):

$$N(z) = N(0) + G_N \left[z - D_p \frac{\left(\frac{z+z_0}{z_0}\right)^p - 1}{p} \right] \quad (4)$$

The parameters D_p and p are linked by a relationship identical to 3, δ being now equal to $-Z_c$.

III. Analytical Approximation of the PIRAM Profile

We ran our "*bulk*" model PIRAM nearly 5000 times with various input meteorological situations. More precisely, we choose our inputs as follows:

- Sea temperature ∈ [5°C ; 25°C]
- Air Sea Temperature Difference, ASTD∈ [-8°C ; 0°C]
- Relative Humidity ∈ [40 % ; 95 %]
- Wind Speed ∈ [1 m/s ; 18 m/s]
- The atmospheric pressure was fixed at 1013 hPa.

With a methodology very similar to the one described in [2], we fitted each PIRAM profile with the expression (4), our fitting criteria being to minimize the Root Mean Square Error (RMSE). We performed two different fitting processes, one working directly with the *N* profile and the other using the *dN/dz* vertical gradient. The two fits produce quite similar profiles with very low RMSE values. An example is plotted in Fig. 2. It corresponds to an ASTD of -5°C and the data set is issued from the MAPTIP trial [4].

IV. Ray Tracing Results

During the MAPTIP campaign, unstable atmospheric conditions prevailed resulting in subrefraction effects: reduction of the optical horizon compared to the standard one and mirage effects just below the horizon (a target can be seen under two different elevation angles). Visible and IR cameras monitored continuously a ship displacement and thus measured the extension of the mirage zone. Various publications such as [4] indicate that these mirage effects are described with good accuracy by bulk profiles coupled with ray tracing algorithms. For the particular data used in Fig. 2, the corresponding computed mirage zone is shown in Fig. 3. We computed these mirage zones by using the PIRAM bulk profile and the analytical fitted ones. The resulting differences were less than 100 m. Such very closed simulation results were obtained for other atmospheric situations corresponding to various ASTD values.

Finally, we can conclude that (2) and (4) constitute a set of expressions enabling to precisely describe a surface layer refractivity profiles for ducting situations as well as for subrefraction cases.

References

[1] S. J. Salamon, H. J. Hansen and D. Abbott, "Modelling radio refractive index in the atmospheric surface layer," Elec. Let., 9th July 2015, Vol 51, N°14, pp. 1119-1121.

[2] J. Claverie and Y. Hurtaud, "Assessment of an analytical expression for an evaporation duct refractivity profile," 2017 IEEE APS and URSI, 9-14 July, San Diego, DOI: 10.1109/USNC-URSI.2017.8074900

[3] J. Claverie and Y. Hurtaud, "Statistical study of EO propagation parameters in coastal areas," Optics in atmospheric propagation and adaptive systems V, 22-27 Sept. 2002, Proceedings SPIE 4884-24, pp 140-148, ISBN 0-8194-4666-1.

[4] J.L. Forand, D. Dion and J. Beaulieu, "MAPTIP: Canada's measurements of refraction effects," AGARD-CP-567, pp 24-1 ; 24-7, 1995.

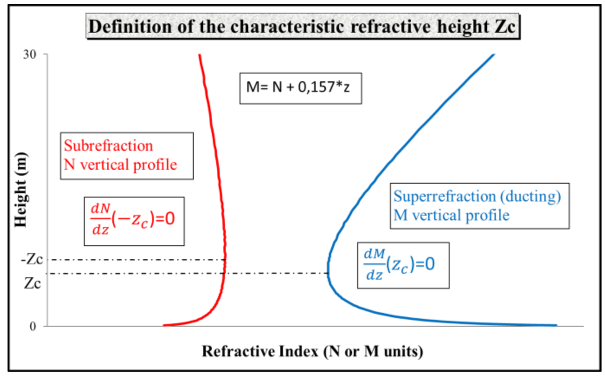

Fig. 1. Typical refractivity profiles in the MSL illustrating the definition of the Characteristic Refractive Height..

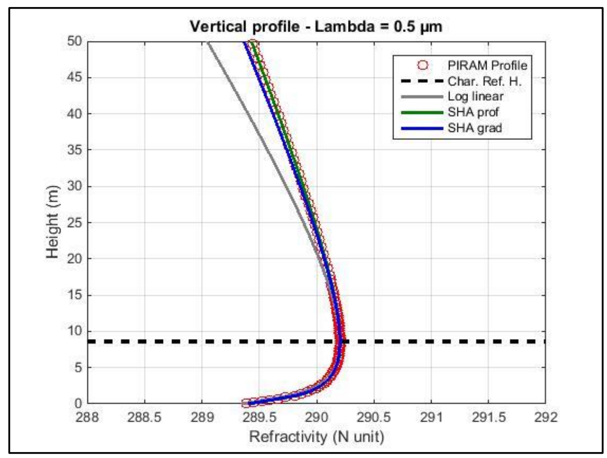

Fig. 2. Example of a PIRAM refractivity profile and the corresponding fitted profiles. This case comes from the MAPTIP dataset and corresponds to an ASTD of -5°C.

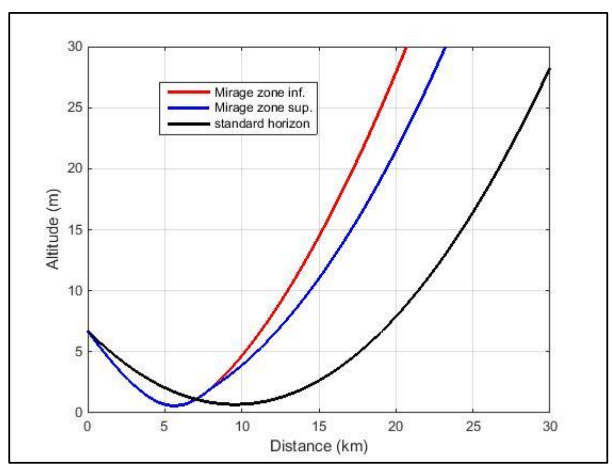

Fig. 3. Mirage zone computed with the refractivity profile of Fig. [2]. The optical sensor (visible camera) was quite at 7m above the sea level.